

# Global fits to $D^0$ CPV parameters using an HFAG like fit

R. Andreassen<sup>1</sup>, A. Davis<sup>1</sup>, M.D. Sokoloff<sup>1</sup>

<sup>1</sup>*University of Cincinnati*

## Abstract

The new  $D^0 \rightarrow K\pi$  result from LHCb provides a credibly powerful constraint on mixing parameters. This note describes a fit in the style of HFAG to combine our result with previous measurements.

# Contents

<b>1</b>	<b>Introduction</b>	<b>1</b>
<b>2</b>	<b>Chi-square calculation</b>	<b>1</b>
<b>3</b>	<b>Fit variants</b>	<b>2</b>
<b>4</b>	<b>Measurements Used</b>	<b>4</b>
<b>5</b>	<b>Results</b>	<b>4</b>
5.1	No CP Violation Allowed . . . . .	4
5.2	No Direct CP Violation Allowed . . . . .	6
5.3	All CP Violation Allowed . . . . .	7
<b>6</b>	<b>Conclusion</b>	<b>7</b>

## 1 Introduction

To fully understand the global impact of the updated WS  $D^0 \rightarrow K\pi$  analysis, a combination of global results of the neutral  $D$  system is necessary. We present an HFAG-like fit for the underlying parameters  $|q/p|$ ,  $\phi$ ,  $x$  and  $y$  using the updated 2011+2012 LHCb  $D^0 \rightarrow K\pi$  results.

## 2 Chi-square calculation

The purpose of our fit is to combine the errors on several different measurements of the same parameters, where each measurement may have a different relation to the underlying true mixing parameters (eg measuring  $(x'^2, y')$  in place of  $(x, y)$ ), and where the numbers in each measurement may be strongly correlated. To do so we construct an overall  $\chi^2$  for all the results:

$$\chi^2 = \vec{\epsilon}^T \sigma^{-1} \vec{\epsilon} \quad (1)$$

where the elements of  $\vec{\epsilon}$  are given by  $\epsilon_i = m_i - p_i$ . Here  $\vec{m}$  is the list of measured values from experiments, and  $\vec{p}$  is a set of “proposed” values for the mixing parameters; we use MINUIT to vary  $\vec{p}$  so as to minimise  $\chi^2$ . Finally,  $\sigma$  is an  $N \times N$  matrix where  $N$  is the number of measurements, with  $\sigma_{ij} = e_i c_{ij} e_j$ . Here  $e_i$  is the reported error on measurement  $i$ , and  $c_{ij}$  is the correlation coefficient between measurements  $i$  and  $j$ .

Notice that, if the measurements are uncorrelated, then  $\sigma$  reduces to a diagonal matrix where the elements are the squares of the measurement errors. In this case  $\chi^2$  is simply the sum  $\sum_i \epsilon_i^2 / e_i^2$ , that is, each element is the difference between a measurement and the corresponding prediction, divided by the error on the measurement, squared. In other words, if there are no correlations we recover the usual chi-square goodness-of-fit metric.

### 3 Fit variants

In full generality, we wish to fit for no less than seven underlying related mixing parameters:

- $x$  and  $y$ , the normalised mass and width differences
- $R_D^+$  and  $R_D^-$ , the ratios of rates
- $\delta$ , the strong phase difference
- $|q/p|$  and  $\phi$ , the magnitude and phase of the indirect CP violation.

The observed inputs, however, are not all direct measurements of these quantities. From  $D^0 \rightarrow K_S \pi \pi$  we get direct measurements of  $x$ ,  $y$ ,  $|q/p|$  and  $\phi$ ;  $D^0 \rightarrow K \pi$  results also yield  $R_D^\pm$  directly, although sometimes quoted as  $R_D = \frac{1}{2}(R_D^+ + R_D^-)$  and  $A_D = \frac{R_D^+ - R_D^-}{R_D^+ + R_D^-}$ . However, we also measure the derived parameters  $x'^{2(\pm)}$ ,  $y'^{(\pm)}$ ,  $y_{CP}$ , and  $A_\Gamma$ , defined as:

$$x' = x \cos \delta + y \sin \delta \quad (2)$$

$$y' = y \cos \delta - x \sin \delta \quad (3)$$

$$x'^{\pm} = \left( \frac{1 \pm A_M}{1 \mp A_M} \right)^{1/4} (x' \cos \phi \pm y' \sin \phi) \quad (4)$$

$$y'^{\pm} = \left( \frac{1 \pm A_M}{1 \mp A_M} \right)^{1/4} (y' \cos \phi \mp x' \sin \phi) \quad (5)$$

$$2y_{CP} = (|q/p| + |p/q|) y \cos \phi - (|q/p| - |p/q|) x \sin \phi \quad (6)$$

$$2A_\Gamma = (|q/p| - |p/q|) y \cos \phi - (|q/p| + |p/q|) x \sin \phi \quad (7)$$

$$(8)$$

where the helper quantity  $A_M$  is given by

$$A_M = \frac{|q/p|^2 - |p/q|^2}{|q/p|^2 + |p/q|^2}. \quad (9)$$

To calculate  $\vec{\epsilon}$ , then, we take in a vector of proposed mixing parameters from MINUIT, calculate the resulting observable parameters from the equations above, and subtract the actually observed numbers.

In addition to the fully-general fit allowing all these variables to float, there are some variants imposing different no-CPV constraints:

- No CP violation. In this fit we set  $|q/p| = 1$ ,  $\phi = 0$ , and  $R_D^+ = R_D^-$ , and fit only for  $x$ ,  $y$ ,  $\delta$ , and  $R_D$ .
- No direct CP violation. With no direct CP violation,  $R_D^+ = R_D^-$ ; in addition, the four parameters  $x$ ,  $y$ ,  $\phi$  and  $|q/p|$  are related (in the limit that CPV is small) by the

42 constraint

$$|q/p| = 1 - \frac{y}{x} \tan \phi \quad (10)$$

$$\phi = \tan^{-1} \left( \frac{1 - |q/p|^2 \frac{x}{y}}{1 + |q/p|^2 \frac{x}{y}} \right) \quad (11)$$

43 Thus we have two variants on this fit:

44 **2a** Here we allow  $|q/p|$  to float and calculate  $\phi$  from the constraint.

45 **2b** We allow  $\phi$  to float and calculate  $|q/p|$  from the constraint.

46 • All CPV allowed. As  $A_D$  is quite small, the contribution of a new physics phase to  $\phi$   
 47 is far below our current sensitivity; consequently the constraint above is a reasonable  
 48 approximation. We therefore run three variants of the all-CPV-allowed scenario:

49 **3a** All parameters float, no constraint.

50 **3b**  $\phi$  is calculated from  $|q/p|$  as above, rather than allowed to float.  $R_D^+$  and  $R_D^-$  are  
 51 both free, as before.

52 **3c** As in 3b, but with  $|q/p|$  calculated from the constraint and  $\phi$  allowed to float.

53 In addition, we do a fit not allowing direct CP violation, in which the free parameters  
 54 are the underlying<sup>1</sup>  $x_{12}$ ,  $y_{12}$ , and  $\phi$ . These parameters are related (in the limit of no direct  
 55 CP violation) to  $|q/p|$ ,  $x$ ,  $y$  and  $\phi$  (no subscripts!) as follows:

$$x = \frac{1}{\sqrt{2}} \text{sg}(\cos \phi_{12}) \sqrt{x_{12}^2 - y_{12}^2 + |x_{12}^2 + y_{12}^2| - 4x_{12}^2 y_{12}^2 \sin^2(\phi_{12})} \quad (12)$$

$$y = \frac{1}{\sqrt{2}} \sqrt{y_{12}^2 - x_{12}^2 + |x_{12}^2 + y_{12}^2| - 4x_{12}^2 y_{12}^2 \sin^2(\phi_{12})} \quad (13)$$

$$|q/p| = \left( \frac{x_{12}^2 + y_{12}^2 + 2x_{12}y_{12} \sin(\phi_{12})}{x_{12}^2 + y_{12}^2 - 2x_{12}y_{12} \sin(\phi_{12})} \right)^{1/4} \quad (14)$$

$$\phi = -\frac{1}{2} \frac{\sin(2\phi_{12})}{\cos(2\phi_{12}) + \frac{y_{12}^2}{x_{12}^2}}. \quad (15)$$

56 Our approach in this fit is to allow MINUIT to believe that the parameters  $x_{12}$ ,  $y_{12}$ , and  
 57  $\phi_{12}$  are free, but interpret them internally as giving rise to the non-underlying parameters  
 58  $x$ ,  $y$ ,  $\phi$ , and  $|q/p|$ , and use these values in the calculation of  $\chi^2$ , as outlined for the other  
 59 fits.

---

<sup>1</sup>See Kagan and Sokoloff, <http://arxiv.org/abs/0907.3917>.

## 4 Measurements Used

Of all of the current measurements available, only a few are resonable for certain fits. Table 1 lists all the possible measurements pertaining to fits excluding CP Violation. Table ?? corresponds to measurements allowing only direct CP violation, and Table ?? lists all measurments pertaining to both direct and indirect CP violation allowed.

Table 1: No CPV allowed inputs

Result	Value	Correlation Coefficients
HFAG $y_{cp}$	$0.00866 \pm 0.00155 \pm 0$	
LHCb $x'^2(K\pi)$	$5.5e - 05 \pm 4.2e - 05 \pm 2.6e - 05$	
LHCb $y'(K\pi)$	$0.00481 \pm 0.00085 \pm 0.00053$	
LHCb $R_D$	$0.003568 \pm 5.8e - 05 \pm 3.3e - 05$	
HFAG $x(K_S^0\pi\pi)$	$0.00419 \pm 0.00211 \pm 0$	
HFAG $y(K_S^0\pi\pi)$	$0.00456 \pm 0.00186 \pm 0$	
CLEO $\cos(\delta)(K\pi)$	$0.81 \pm 0.2 \pm 0.06$	
CLEO $\sin(\delta)(K\pi)$	$-0.01 \pm 0.41 \pm 0.04$	
CDF $R_D$	$0.00304 \pm 0.00055 \pm 0$	
CDF $x'^2(K\pi)$	$-0.00012 \pm 0.00035 \pm 0$	
CDF $y'(K\pi)$	$0.0085 \pm 0.0076 \pm 0$	
Belle $R_D$	$0.00364 \pm 0.00017 \pm 0$	
Belle $x'^2(K\pi)$	$0.00018 \pm 0.00022 \pm 0$	
Belle $y'(K\pi)$	$0.0006 \pm 0.004 \pm 0$	
BaBar $R_D$	$0.00303 \pm 0.00016 \pm 0.0001$	
BaBar $x'^2(K\pi)$	$-0.00022 \pm 0.0003 \pm 0.00021$	
BaBar $y'(K\pi)$	$0.0097 \pm 0.0044 \pm 0.0031$	

## 5 Results

The results are split into subsections depending on the type of CP Violation allowed. Additonally, results are presented using a variety of different combinations of the available data. Figure 1 shows all variations for the no CPV allowed fits. Figure 3 shows the results for a subset of variations on All CPV allowed fits.

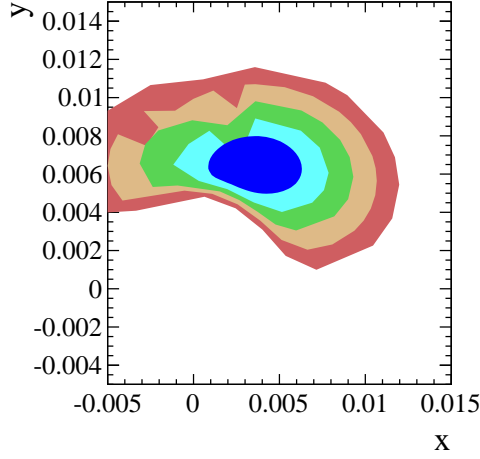
### 5.1 No CP Violation Allowed

Table 4 lists the results from the No CP Violation allowed global fit. As  $A_\Gamma = 0$  in the the case of No CPV, the data is not included in this fit. Additionally, we take subsets of

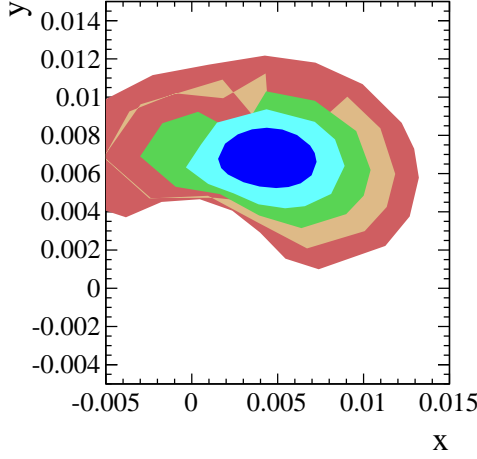
Table 2: No Direct CPV allowed inputs

Result	Value	Correlation Coefficients
HFAG $y_{CP}$	$0.00866 \pm 0.00155 \pm 0$	
HFAG $A_\Gamma$	$-0.00022 \pm 0.00161 \pm 0$	
LHCb $A_\Gamma(KK)$	$-0.00035 \pm 0.00062 \pm 0.00012$	
LHCb $A_\Gamma(\pi\pi)$	$0.00033 \pm 0.00106 \pm 0.00014$	
LHCb $R_D$	$0.003568 \pm 5.8e-05 \pm 3.3e-05$	
LHCb $y'^+(K\pi)$	$0.00446 \pm 0.00089 \pm 0.00057$	
LHCb $x'^{2+}(K\pi)$	$7.7e-05 \pm 4.6e-05 \pm 2.9e-05$	
LHCb $y'^-(K\pi)$	$0.00517 \pm 0.00089 \pm 0.00058$	
LHCb $x'^{2-}(K\pi)$	$3.2e-05 \pm 4.7e-05 \pm 3e-05$	
Belle $x(K_S^0\pi\pi)$	$0.00811 \pm 0.00334 \pm 0$	
Belle $y(K_S^0\pi\pi)$	$0.00309 \pm 0.00281 \pm 0$	
Belle $ q/p $	$0.95 \pm 0.22 \pm 0.1$	
Belle $\phi$	$-0.035 \pm 0.19 \pm 0.09$	
CLEO $\cos(\delta)(K\pi)$	$0.81 \pm 0.2 \pm 0.06$	
CLEO $\sin(\delta)(K\pi)$	$-0.01 \pm 0.41 \pm 0.04$	
CLEO $R_D$	$0.00533 \pm 0.00107 \pm 0.00045$	
CLEO $x'^2(K\pi)$	$0.0006 \pm 0.0023 \pm 0.0011$	
CLEO $y'(K\pi)$	$0.042 \pm 0.02 \pm 0.01$	
CDF $R_D$	$0.00304 \pm 0.00055 \pm 0$	
CDF $x'^2(K\pi)$	$-0.00012 \pm 0.00035 \pm 0$	
CDF $y_{prime}(K\pi)$	$0.0085 \pm 0.0076 \pm 0$	
Belle $R_D$	$0.00364 \pm 0.00018 \pm 0$	
Belle $x'^{2-}(K\pi)$	$6e-05 \pm 0.00034 \pm 0$	
Belle $y'^-(K\pi)$	$0.002 \pm 0.0054 \pm 0$	
Belle $x'^{2+}(K\pi)$	$0.00032 \pm 0.00037 \pm 0$	
Belle $y'^+(K\pi)$	$-0.0012 \pm 0.0058 \pm 0$	
BaBar $R_D$	$0.00303 \pm 0.000189 \pm 0$	
BaBar $x'^{2-}(K\pi)$	$-0.0002 \pm 0.0005 \pm 0$	
BaBar $y'^-(K\pi)$	$0.0096 \pm 0.0075 \pm 0$	
BaBar $x'^{2+}(K\pi)$	$-0.00024 \pm 0.00052 \pm 0$	
BaBar $y'^+(K\pi)$	$0.0098 \pm 0.0078 \pm 0$	
BaBar $x(K_S^0\pi\pi)$	$0.0016 \pm 0.0023 \pm 0.0012$	
BaBar $y(K_S^0\pi\pi)$	$0.0057 \pm 0.002 \pm 0.0013$	

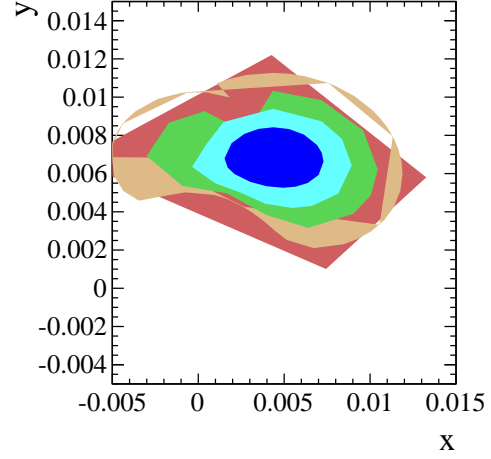
<sup>73</sup> the data which do not include results from Belle, BaBar and CDF in order to explore the  
<sup>74</sup> change in  $\chi^2/\text{ndf}$  of the global fit.



(a) Two dimensional error ellipses for  $x$  and  $y$  using all available measurements.



(b) Two dimensional error ellipses for  $x$  and  $y$  from fit excluding Belle and BaBar  $K\pi$  results.



(c) Two dimensional error ellipses for  $x$  and  $y$  from fit excluding Belle, BaBar and CDF measurements.

Figure 1: Two dimensional error ellipses of  $x$  and  $y$  from fit for No CPV. Exclusion of the Belle and BaBar results drastically change the slope of the error ellipses. The differing colors represent the 1-5 $\sigma$  contours.

## 5.2 No Direct CP Violation Allowed

Table 5 lists the results of the global fit of no direct CP violation. The final three columns of the table represent the effect of the inclusion of the preliminary LHCb  $A_F$  result in the global fit. The inclusion of this result does not change the central values or errors

79 substantially.

### 80 5.3 All CP Violation Allowed

81 Table 6 lists the results of the global All CP Violation allowed fit. Again, the latter  
82 columns list the differing subsets of the data to explore the variation in global  $\chi^2/\text{ndf}$ .  
83 The most noticable difference between all fits is the evaluation of  $x$ , which varies quite a  
84 bit with the inclusion of differing datasets.

## 85 6 Conclusion

86 By utilizing a global, HFAG-like fit, we constrain to be  $|q/p| = xxxxx \pm yyyyy$  and  
87  $\phi = zzzzzzz \pm qqqqqqqqqqqq$ , in the case of all CPV allowed. Allowing only direct CPV,  
88  $|q/p| = xxxxx \pm yyyyy$  and  $\phi = zzzzzzz \pm qqqqqqqqqqqq$ . These measurements represent  
89 the most precise determination of the CP violating parameters of the natural  $D$  meson  
90 system



Table 3: All CPV allowed inputs

Result	Value	Correlation Coefficients
HFAG $y_{CP}$	$0.00866 \pm 0.00155 \pm 0$	
HFAG $A_\Gamma$	$-0.00022 \pm 0.00161 \pm 0$	
LHCb $A_\Gamma(KK)$ LHCb $A_\Gamma(\pi\pi)$	$-0.00035 \pm 0.00062 \pm 0.00012$ $0.00033 \pm 0.00106 \pm 0.00014$	
LHCb $x'^{2+}(K\pi)$ LHCb $y'^+(K\pi)$ LHCb $R_D^+$ LHCb $x'^{2-}(K\pi)$ LHCb $y'^-(K\pi)$ LHCb $R_D^-$	$5.5e-05 \pm 4.2e-05 \pm 2.6e-05$ $0.00481 \pm 0.00085 \pm 0.00053$ $0.003568 \pm 5.8e-05 \pm 3.3e-05$ $5.5e-05 \pm 4.2e-05 \pm 2.6e-05$ $0.00481 \pm 0.00085 \pm 0.00053$ $0.003568 \pm 5.8e-05 \pm 3.3e-05$	
Belle $x(K_S^0\pi\pi)$ Belle $y(K_S^0\pi\pi)$ Belle $ q/p $ Belle $\phi$	$0.0081 \pm 0.003 \pm 0.0015$ $0.0037 \pm 0.0025 \pm 0.0012$ $0.86 \pm 0.3 \pm 0.1$ $-0.244 \pm 0.31 \pm 0.09$	
CLEO $\cos(\delta)(K\pi)$ CLEO $\sin(\delta)(K\pi)$ CLEO $R_D$ CLEO $x'^2(K\pi)$ CLEO $y'(K\pi)$	$0.81 \pm 0.2 \pm 0.06$ $-0.01 \pm 0.41 \pm 0.04$ $0.00533 \pm 0.00107 \pm 0.00045$ $0.0006 \pm 0.0023 \pm 0.0011$ $0.042 \pm 0.02 \pm 0.01$	
CDF $R_D$ CDF $x'^2(K\pi)$ CDF $y'(K\pi)$	$0.00304 \pm 0.00055 \pm 0$ $-0.00012 \pm 0.00035 \pm 0$ $0.0085 \pm 0.0076 \pm 0$	
Belle $R_D^-$ Belle $x'^{2-}(K\pi)$ Belle $y'^-(K\pi)$ Belle $R_D^+$ Belle $x'^{2+}(K\pi)$ Belle $y'^+(K\pi)$	$0.0036 \pm 0.0002 \pm 0$ $6e-05 \pm 0.00034 \pm 0$ $0.002 \pm 0.0054 \pm 0$ $0.00368 \pm 0.0002 \pm 0$ $0.00032 \pm 0.00037 \pm 0$ $-0.0012 \pm 0.0058 \pm 0$	
BaBar $R_D^-$ BaBar $x'^{2-}(K\pi)$ BaBar $y'^-(K\pi)$ BaBar $R_D^+$ BaBar $x'^{2+}(K\pi)$ BaBar $y'^+(K\pi)$	$0.00303 \pm 0.0002 \pm 0.0001$ $-0.0002 \pm 0.00041 \pm 0.00029$ $0.0096 \pm 0.0064 \pm 0.0045$ $0.00303 \pm 0.0002 \pm 0.0001$ $-0.00024 \pm 0.00043 \pm 0.0003$ $0.0098 \pm 0.0061 \pm 0.0043$	
BaBar $x(K_S^0\pi\pi)$ BaBar $y(K_S^0\pi\pi)$	$0.0016 \pm 0.0023 \pm 0.0012$ $0.0057 \pm 0.002 \pm 0.0013$	

	All Results	No Belle, BaBar	No Belle, BaBar, CDF
$x(\times 10^{-3})$	$3.677 \pm 1.815$	$4.497 \pm 1.912$	$4.515 \pm 1.919$
$y(\times 10^{-3})$	$6.504 \pm 1.006$	$6.856 \pm 1.040$	$6.876 \pm 1.041$
$\delta_{K\pi}(\times 10^{-1})$	$2.210 \pm 2.638$	$3.3407 \pm 2.131$	$3.253 \pm 2.141$
$R_D(\times 10^{-3})$	$3.497 \pm 0.041$	$3.552 \pm 0.046$	$3.552 \pm 0.047$
$\chi^2/ndf$	34.5065/13	14.8181/7	4.04354/4

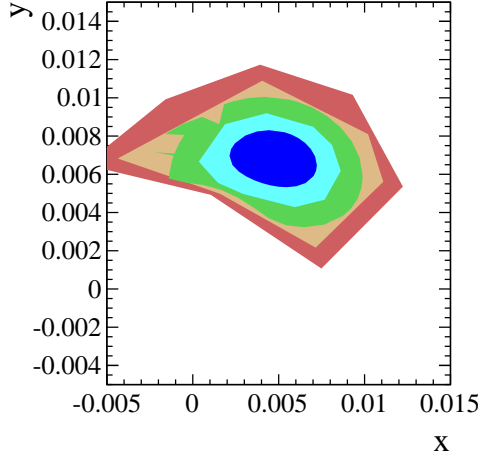
Table 4: Output values of No CPV allowed global fit. Different columns list subsets of allowed data.

	All Measurements	No Belle, BaBar	No Belle, BaBar, $A_{\Gamma \text{ LHCb}}$	No Belle, BaBar, CDF, $A_{\Gamma \text{ LHCb}}$
$x(\times 10^{-3})$	$5.111 \pm 1.779$	$4.843 \pm 1.782$	$4.845 \pm 1.782$	$4.844 \pm 1.787$
$y(\times 10^{-3})$	$6.891 \pm 1.033$	$6.797 \pm 1.029$	$6.797 \pm 1.030$	$6.809 \pm 1.031$
$\delta_{K\pi}(\times 10^{-1})[\text{rad}]$	$3.529 \pm 1.897$	$3.187 \pm 2.021$	$3.188 \pm 2.021$	$3.084 \pm 2.040$
$R_D(\times 10^{-3})$	$3.583 \pm 0.046$	$3.555 \pm 0.046$	$3.556 \pm 0.046$	$3.556 \pm 0.047$
$ q/p (\times 10^{-1})$	$9.931 \pm 0.125$	$9.935 \pm 0.135$	$9.929 \pm 0.131$	$9.930 \pm 0.130$
$\chi^2/ndf$	14.6697/25	19.0559/13	19.3925/15	8.61793/12

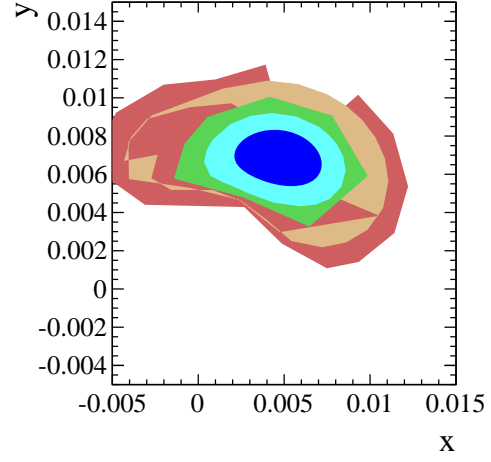
Table 5: Output values of No Direct CPV allowed global fit. Different columns list subsets of allowed data.

	All Measurements	No Belle, BaBar	No Belle, BaBar, $A_{\Gamma \text{ LHCb}}$	No Belle, BaBar, CDF, $A_{\Gamma \text{ LHCb}}$
$x(\times 10^{-3})$	$3.703 \pm 1.637$	$4.817 \pm 1.688$	$4.772 \pm 1.685$	$4.601 \pm 1.664$
$y(\times 10^{-3})$	$6.424 \pm 0.925$	$6.868 \pm 0.984$	$6.908 \pm 0.963$	$6.956 \pm 0.867$
$\delta_{K\pi}(\times 10^{-1})[\text{rad}]$	$1.983 \pm 2.452$	$3.246 \pm 1.935$	$3.329 \pm 1.891$	$3.250 \pm 1.756$
$\phi(\times 10^{-1})[\text{rad}]$	$-0.645 \pm 1.193$	$-0.623 \pm 1.055$	$-0.651 \pm 1.046$	$-1.534 \pm 1.712$
$R_D(\times 10^{-3})$	$3.507 \pm 0.042$	$3.568 \pm 0.049$	$3.567 \pm 0.049$	$3.582 \pm 0.055$
$R_D^+(\times 10^{-3})$	$3.500 \pm 0.037$	$3.547 \pm 0.044$	$3.548 \pm 0.043$	$3.533 \pm 0.046$
$ q/p (\times 10^{-1})$	$9.601 \pm 0.706$	$9.513 \pm 0.823$	$9.474 \pm 0.800$	$8.880 \pm 1.082$
$\chi^2/ndf$	50.4281/26	18.8317/11	19.1817/14	7.72181/9

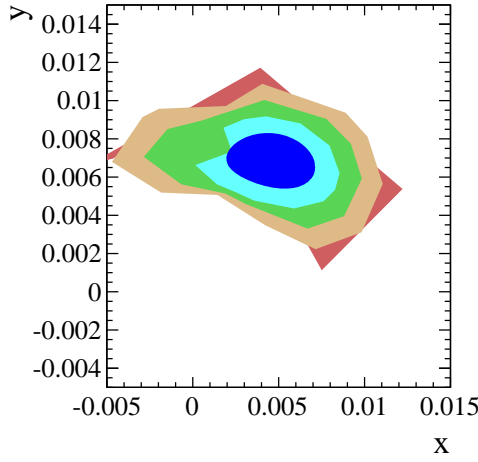
Table 6: Output of the All CP Violation allowed global fit. Different Columns list differing subsets of data included in the fit.



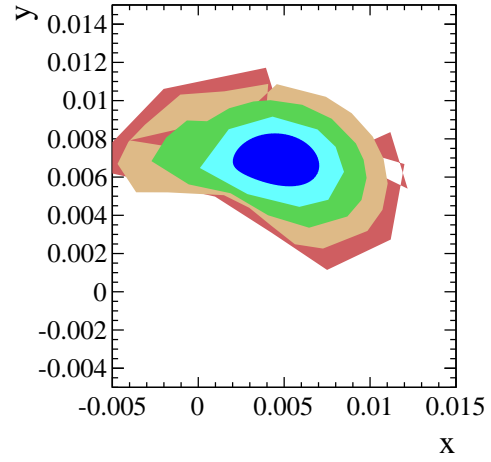
(a) Two dimensional error ellipses for  $x$  and  $y$  from fit excluding Belle and BaBar  $K\pi$  results. Does not include latest  $A_\Gamma$  result of LHCb.



(b) Two dimensional error ellipses for  $x$  and  $y$  from fit excluding Belle and BaBar  $K\pi$  results. Include latest  $A_\Gamma$  result of LHCb.

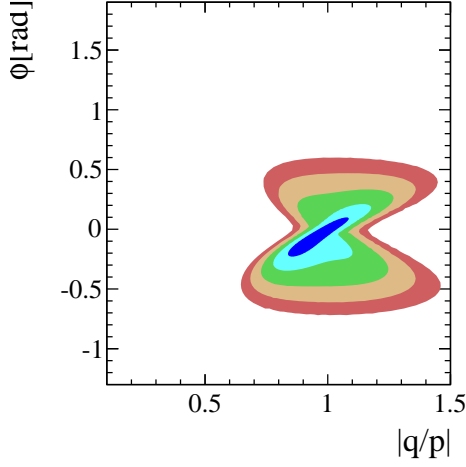


(c) Two dimensional error ellipses for  $x$  and  $y$  from fit excluding Belle, BaBar and CDF  $K\pi$  results. Does not include latest  $A_\Gamma$  result of LHCb.

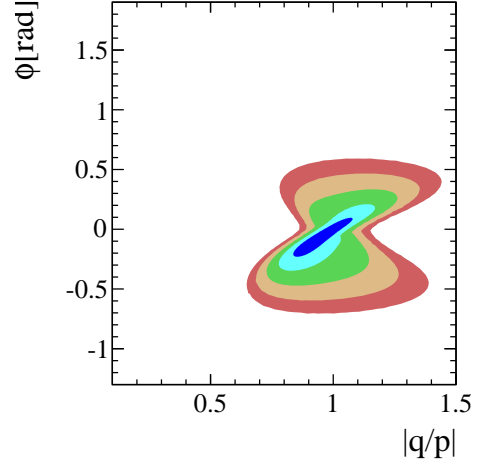


(d) Two dimensional error ellipses for  $x$  and  $y$  from fit excluding Belle, BaBar and CDF  $K\pi$  results. Include latest  $A_\Gamma$  result of LHCb.

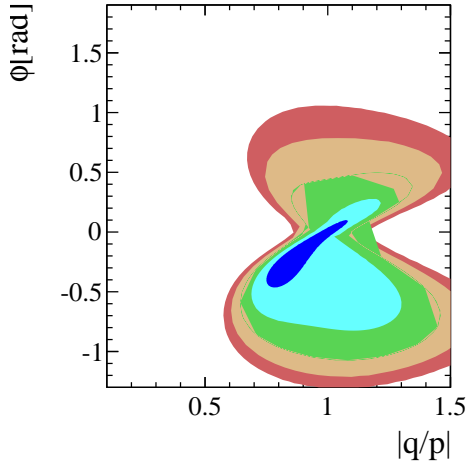
Figure 2: Two dimensional error ellipses of fit for All CPV including differing sets of data for  $x$  vs  $y$ . The biggest differences come from including the CDF result, which elongates the error ellipses. The differing colors represent the 1-5 $\sigma$  contours.



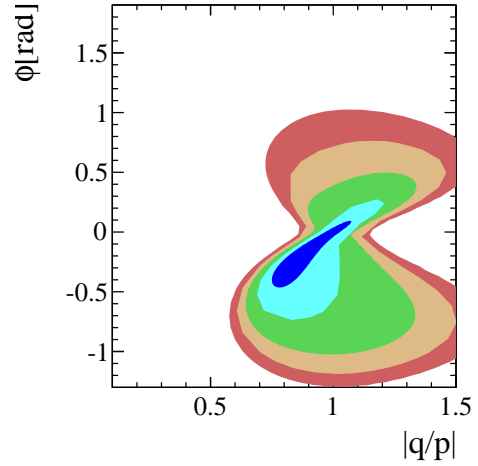
(a) Two dimensional error ellipses for  $x$  and  $y$  from fit excluding Belle and BaBar  $K\pi$  results. Does not include latest  $A_\Gamma$  result of LHCb.



(b) Two dimensional error ellipses for  $x$  and  $y$  from fit excluding Belle and BaBar  $K\pi$  results. Include latest  $A_\Gamma$  result of LHCb.



(c) Two dimensional error ellipses for  $x$  and  $y$  from fit excluding Belle, BaBar and CDF  $K\pi$  results. Does not include latest  $A_\Gamma$  result of LHCb.



(d) Two dimensional error ellipses for  $x$  and  $y$  from fit excluding Belle, BaBar and CDF  $K\pi$  results. Include latest  $A_\Gamma$  result of LHCb.

Figure 3: Two dimensional error ellipses of fit for All CPV including differing sets of data for  $\phi$  vs  $q/p$ . The biggest differences come from including the CDF result, which elongates the error ellipses. The differing colors represent the 1-5 $\sigma$  contours.